6-2011

A feature based frequency domain analysis algorithm for fault detection of induction motors

Zhaoxia WANG
Singapore Management University, zxwang@smu.edu.sg

C. S. CHANG

ZHANG Yifan

Published in 2011 6th IEEE Conference on Industrial Electronics and Applications ICIEA: June 21-23, Beijing: Proceedings, pp. 27-32.
DOI: 10.1109/ICIEA.2011.5975545

A Feature Based Frequency Domain Analysis Algorithm for Fault Detection of Induction Motors

Zhaoxia Wang
Department of Computer Science,
Institute of High Performance Computing (IHPC),
Singapore 138623.
Email: wangz@ihpc.a-star.edu.sg

C.S. Chang*,Yifan Zhang
Department of Electrical and Computer Engineering,
National University of Singapore (NUS),
Singapore 117576
Email: eleccs@nus.edu.sg

***Abstract*—This paper studies the stator currents collected from several inverter-fed laboratory induction motors and proposes a new feature based frequency domain analysis method for performing the detection of induction motor faults, such as the broken rotor-bar or bearing fault. The mathematical formulation is presented to calculate the features, which are called FFT-ICA features in this paper. The obtained FFT-ICA features are normalized by using healthy motor as benchmarks to establish a feature database for fault detection. Compare with conventional frequency-domain analysis method, no prior knowledge of the motor parameters or other measurements are required for calculating features. Only one phase stator current waveforms are enough to provide consistent diagnosis of inverter-fed induction motors at different frequencies. The proposed method also outperforms our previous time domain analysis method.**

***Index Terms*—Fault detection, Fast Fourier Transform, Induction motors fed from inverter, Independent Component Analysis.**

I. Introduction

Stator-current monitoring is viewed as an important fault-detection scheme without requiring special access to the motor [1]. Current signals from faulty motors can show essential difference from those in the normal condition [1]. There is a significant amount of research in this area, and broken rotor-bars and bearing faults are two main fault types in induction motors [1]–[4], where most research was performed by decomposing and analyzing stator currents using various methods such as Fourier analysis, wavelets, neural networks, model-based techniques, and other statistical analysis [5]–[15].

Many of these methods are influenced by factors arising from electric supply, noise, and fault conditions, some of which may lead to erroneous fault detection [16]–[18].

Independent component analysis (ICA) is a powerful computational algorithm for automatically separating a multivariate signal into additive subcomponents by exploiting the mutual statistical independence of non-Gaussian source signals [12]–[14], [19]–[21]. It is a special case of blind source separation, and has many practical applications such as signal processing [22] and biomedical engineering [23]. ICA captures the essential structure of the data in many applications, including feature extraction and signal separation because of its property of extracting statistically independent components.

ICA has been recently used for fault detection of induction motors [12], [14], [24]. One such research applies ICA and support vector machines for fault diagnosis of induction motors [24] using vibration signals collected at the vertical, horizontal and axial positions and current signals over the three phases. A total of 78 features are extracted in the time domain for deriving 10 feature parameters. Three other parameters are extracted from the frequency domain separately in this research.

We propose a feature based frequency domain analysis method that exploits the relative strengths of frequency-domain analysis and ICA by applying ICA on frequency-domain signals. As revealed in our previous work [12], [14], healthy or faulty motors each exhibits unique signatures in the frequency domain more than in the time domain. As frequency-domain signatures are rich in information content, only a few features need to be extracted from a moderate volume of signals for making consistent fault detection on induction motors. Accordingly, ICA is applied to frequency-domain signatures for identifying the dominant independent components to maintain a simple fault classifier by removing less dominant ones. Our proposed algorithm has also an important advantage of not requiring any prior knowledge of motor/ bearing mechanical and electrical parameters in any fault detection. Therefore, ICA eliminates all human preparation and input of motor/ bearing mechanical and electrical parameters as required by many frequency analysis techniques [1], [8], [9], [11], and greatly enhances the accuracy and efficiency of fault detection of induction motor.

This paper is divided into four sections. Section II provides the literature review of conventional frequency-domain analysis method. Section III presents the setup for collecting diagnostic data from laboratory induction motors. Section IV presents our proposed FFT-ICA scheme which includes mathematical formulation of the proposed algorithm, performance of the proposed algorithm compared with conventional frequency-domain analysis method and our previous time-domain method. Section V concludes the paper.

II. Conventional Frequency-Domain Analysis Methods

A. Frequency-Domain Fault Signatures

Among the many techniques developed for motor-current signature analysis (MCSA) [1]–[4], [8]–[15], FFT is the most

widely used tool. FFT decomposes a time domain into components of different frequencies. Motor stator current acts as an excellent transducer for detecting faults in motors. During operation, many harmonics will be present in a motor signal. FFT spectrum will thus show many peaks, including the inverter (fundamental) frequency and its harmonics. This is known as the motor current signatures. Current signatures of faulty motors differ from those of healthy motors, because different electrical and mechanical faults generate different harmonics.

Bearing faults take the form of outer-race, inner-race, ball or cage defects, which are the main causes of machine vibrations [1], [16]–[18]. Machine-inductance variations are reflected in the stator current in terms of current harmonics, which provide an indicator of bearing faults associated with mechanical oscillations in the air-gap. Bearing fault current harmonic frequencies $f_{bearing}$ are expressed as [1], [17], [18]:

$$f_{bearing} = |f_s \pm m f_{i,v}| \tag{1}$$

where f_s is the fundamental supply frequency, $m = 1, 2, 3, \ldots$ are the harmonic indexes and $f_{i,v}$ is one of the characteristic vibration frequency due to bearing faults.

$$f_{i,o} = \frac{n}{2} f_r \left[1 \pm \frac{bd}{pd} \cos\alpha\right] \tag{2}$$

where

n	number of bearing balls;
f_r	mechanical rotor speed in Hz;
bd	ball diameter;
pd	bearing pitch diameter;
α	contact angle of the balls on the races.

Further explanation about the bearing faults can be found in [1], [17], [18]. Information about the bearing construction, which can be found in Table I, is required to calculate the exact characteristic frequencies as in Eqn. 2.

A broken rotor-bar can be considered as some form of rotor asymmetry that causes unbalanced currents, decreased average torque and increased torque pulsations [1], [3]–[5], [7], [16], [17]. Monitoring the sidebands f_b around the fundamental harmonic is a widely used approach for diagnosing broken rotor-bars in induction motors in the following [1], [3], [4], [16], [17]:

$$f_b = f_s(1 \pm 2ks), k = 1, 2, 3, ... \tag{3}$$

where

f_s	electrical supply frequency;
s	per-unit slip.

B. Challenges for Classifying Healthy and Fault Motors

The inverter frequency, measured motor speed, and physical parameters of the bearing are required in Eqns. 1 and 2 to calculate the bearing fault frequency. Another parameter as required in Eqn. 1 is the harmonic number "m", which is not readily available. By applying the frequency auto search algorithm [18], the estimated bearing fault signatures, $f_{bearing}$ can be obtained. The bearing fault signature frequencies increase with the inverter frequency.

Accurate values of inverter frequency and measured motor speed are required in Eqn. 3 for calculating the broken rotor-bar frequency.

The broken rotor-bar fault signatures (side-bands) depends on the inverter frequency and slip as shown in Eqn. 3, which compounds the difficulty against using sideband as a robust means of detecting rotor-bar faults under wide ranges of slips and inverter frequency. One significant challenge in the broken-rotor-bar detection is to distinguish its respective sidebands especially under low slip operation.

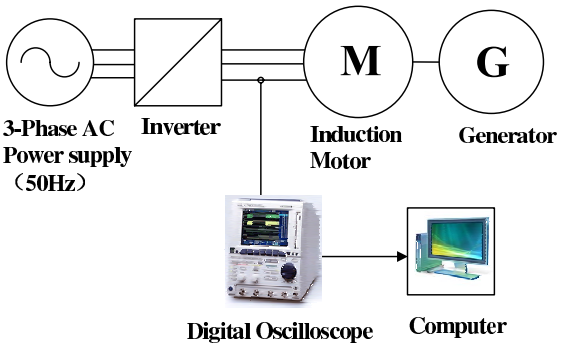

Fig. 1. Laboratory setup for data collection from induction motors

TABLE I
PARAMETERS OF INDUCTION MOTORS FOR DATA COLLECTION

Motor Parameter		Bearing Parameter	
Power	1.1kW	Ball diameter, bd	8.89
Voltage (△/Y)	230/400V	Bearing pitch diameter pd	38.5mm
Current (△/Y)	4.5/2.6A	Number of bearing balls, n	12/13
Frequency	50Hz	Contact angle, α	0°
Speed	1410rpm	Bearing type	NTN-6205Z
Pole pairs	2		

III. EXPERIMENTAL SETUP

Fig. 1 shows our experimental setup for collecting stator-current waveforms from three identical motors of the same technical specifications but with different conditions: one being healthy, one having bearing fault and the other having broken rotor bars [12], [14]. The technical specifications are given in Table I.

Motor faults were artificially created with a dent on the seal, and the deformation of the seal is connected to the inner race of the bearing as shown in Fig. 2(a), and two holes were drilled on the rotor bar of another motor as shown in Fig. 2(b). All induction motors are driven by the same voltage-fed pulse-width modulated inverter on data collection. The healthy motor is considered as a benchmark for comparing with faulty condition.

During data collection, the motors are loaded with a DC generator. Stator currents are measured separately with a 4-channel digital oscilloscope from each of the three motors. The motors are supplied with different frequencies: 20 Hz,

(a)

(b)

Fig. 2. Fault motors: (a) Denting the seal of the bearing to simulate bearing fault; (b) Two holes are drilled on the rotor bar to simulate broken rotor bar.

25 Hz, 37.5 Hz, 43.5 Hz, and 50 Hz. 15 signal segments are collected from each motor at each frequency at the sampling rate of 50 kHz for 20 seconds.

IV. Proposed Feature Based Fault Detection algorithm for Induction-motor Fault Detection

As mentioned in Section II, the fault-signature frequencies of bearing fault and broken rotor-bar are dependent of measurement or parameters of motors.

In this paper, a feature based frequency domain analysis fault detection algorithm is presented. The proposed algorithm does not require above operational dependent information. The necessary information required is stator current signals. The mathematical formula are presented to calculate features. The paper will demonstrate the high accuracy, simplicity and robustness of the proposed algorithm for the fault detection of induction motors run under varying inverter frequency.

A. Mathematical Formulation of the Proposed Feature Based Fault Detection Method

The frequency-domain signal $F(\omega)$ can be obtained from a time-domain waveform $f(t)$ by using FFT:

$$f(t) \rightarrow \begin{pmatrix} f(t_1) & f(t_2) & \cdots & f(t_L) \end{pmatrix} \tag{4}$$

$$F(\omega) = FFT(f(t)) \tag{5}$$

where $f(t_i)(i = 1, 2, \cdots, L)$ is amplitude at time $t_i(i = 1, 2, \cdots, L)$; L is a record length of samples; FFT represents fast Fourier transform function. The frequency-domain signal $F(\omega)$ generated by this transformation includes the magnitude information about each frequency components as the following:

$$F(\omega) \rightarrow \begin{pmatrix} a(\omega_1) & a(\omega_2) & \cdots & a(\omega_N) \end{pmatrix} \tag{6}$$

where $a(\omega_i)(i = 1, 2, \cdots, N)$ is the magnitude of frequency component $\omega_i(i = 1, 2, \cdots, N)$; $\triangle\omega = \omega_{i+1} - \omega_i$ is the resolution selected; N is the selected number of the frequency components.

$F(\omega)$ in Eqn. 6 represents the frequency-domain signal of the healthy motor. From the stator current signals of two faulty motors, $f_{br}(t)$ and $f_{be}(t)$, the frequency-domain signals of the faulty motors, $F_{br}(\omega)$ and $F_{be}(\omega)$ are obtained similarly:

$$F_{br}(\omega) \rightarrow \begin{pmatrix} a_{br}(\omega_1) & a_{br}(\omega_2) & \cdots & a_{br}(\omega_N) \end{pmatrix} \tag{7}$$

$$F_{be}(\omega) \rightarrow \begin{pmatrix} a_{be}(\omega_1) & a_{be}(\omega_2) & \cdots & a_{be}(\omega_N) \end{pmatrix} \tag{8}$$

where $a_{br}(\omega_i)(i = 1, 2, \cdots, N)$ and $a_{be}(\omega_i)(i = 1, 2, \cdots, N)$ are magnitudes of frequency components $\omega_i(i = 1, 2, \cdots, N)$ of broken rotor bar motor and bearing fault motor, respectively.

According to Eqns. 3 and 1, the frequency-domain signal of the broken rotor bar motor has the sidebands around the fundamental harmonics, and the frequency-domain signal of the bearing fault motor is with the signatures of the bearing faults compared with that of the healthy motor. Therefore, Eqns. 6, 7 and 8 can be merged into the following:

$$F\_signals = \begin{pmatrix} a(\omega_1)\cdots a(\omega_n) & \overbrace{0\cdots 0}^{k} & & \overbrace{0\cdots 0}^{m} \\ a(\omega_1)\cdots a(\omega_n) & a(\omega_{br1})\cdots a(\omega_{brk}) & & \overbrace{0\cdots 0}^{m} \\ a(\omega_1)\cdots a(\omega_n) & \overbrace{0\cdots 0}^{k} & a(\omega_{be1})\cdots a(\omega_{bem}) & \end{pmatrix} \tag{9}$$

The first row of Eqn. 9 represents the magnitudes of different frequency components about the healthy motor, i.e. the magnitudes of healthy motor frequency signatures. Because the healthy motor is assumed to be ideal normal, the magnitudes of faulty frequency components are zero. Similarly, the second row of Eqn. 9 shows the magnitudes of frequency signatures of broken rotor bar motor, and the magnitudes of bearing fault frequency components are zero. The third row shows the magnitudes of frequency signatures of bearing fault motor, and the magnitudes of broken rotor bar fault frequency components are zero as shown in Eqn. 9.

According to Eqn. 9, different faults make their frequency-domain signals have different frequency signatures, such as A_{br} and A_{be}. The most important observation is that frequency characteristics of healthy or faulty motors are in fact represented by the magnitudes of the frequency components rather than the frequency components themselves. This means that if the frequency components are fundamental constants, only the magnitudes of the frequency components are enough to detect fault from healthy motors according to Eqn. 9 regardless of other information or parameters of the motor.

Therefore, according to above theoretical analysis, this paper proposes a new feature based frequency domain analysis method for performing the detection of induction motor faults, which only uses the magnitudes of the selected frequency components in Eqn. 9.

The time-domain ICA algorithm as in [12]–[14], [19]–[21] is modified for application to the frequency-domain signals (Eqn. 9) as follows:

$$x = A \cdot s \tag{10}$$

$$s = W \cdot x \tag{11}$$

where x is an observed m-dimensional vector, s is an n-dimensional random vector whose components are assumed to be mutually independent, and A is a constant matrix to be estimated; W is the (pseudo) inverse of the matrix A of Eqn. 10, which is known as transformation matrix [12]–[14], [19]–[21].

A set of statistically independent components, ICs, can be extracted from the frequency-domain signals shown as 9 by using the following:

$$ICs = W \cdot F\_Signals \tag{12}$$

The resulting independent components ICs reflect the characteristic of signals $F\_Signals$ in above Eqn. 12 [12]–[14], [21]. Both the obtained ICs and the signals $F\_Signals$ are then used to calculate FFT-ICA features as following:

$$F\_Features = F\_Signals \bullet ICs^T \tag{13}$$

where $F\_Features$ are the FFT-ICA features of signals $F\_Signals$.

The magnitude information of the selected frequency components of healthy and faulty motors all contribute to the FFT-ICA features as shown in Eqn. 13. For example, F_Signal_m is m^{th} frequency domain signal in $F\_Signals$.

$$F\_Signal_m = \begin{pmatrix} a_m(\omega 1) & a_m(\omega 2) & \dots & a_m(\omega N) \end{pmatrix} \tag{14}$$

where $a_m(\omega 1), a_m(\omega 2), \dots, a_m(\omega N)$ represents the magnitude information about frequency component $\omega 1, \omega 2, \dots, \omega N$, respectively.

F_Signal_m is converted to a M-dimension feature (from feature 1 to feature M) by dependent components ICs and using the following equation:

$$\begin{pmatrix} F\_Feature_{m1} & F\_Feature_{m2} & \dots & F\_Feature_{mM} \end{pmatrix} = F\_Signal_m \times \begin{pmatrix} ic_{11} & ic_{12} & \dots & ic_{1M} \\ ic_{21} & ic_{21} & \dots & ic_{2M} \\ \dots & \dots & \dots & \dots \\ ic_{N1} & ic_{N1} & \dots & ic_{NM} \end{pmatrix} \tag{15}$$

where $F\_Feature_{m1},\ F\_Feature_{m2},\ \dots,\ F\_Feature_{mM}$ represent feature 1, feature 2, ..., and feature M of the m^{th} signal F_Signal_m, respectively. F_Signal_m include the magnitude information about each selected frequency component.

As shown in Eqn. 14 and 15, all the magnitude information of the selected frequency components is used to compute the M-dimension feature of the signal. All the M-dimension features of training data from the healthy and faulty motors are exploited for establishing healthy and faulty signature database for detecting of their faults, such as the broken rotor-bar and bearing faults.

TABLE II
CALCULATED FAULT FREQUENCY OF THE MOTOR WITH BEARING FAULT BY USING THE PARAMETERS IN TABLE I

Inverter Frequency (Hz)	Rotor Speed (rpm)	$f_{bearing}$ (Hz)
20.0	584	331.507
25.0	731	414.916
37.5	1098	623.170
43.5	1274	723.097
50.0	1464	830.890

B. Performance of our proposed Method

As mentioned in Section III, stator-current signals are collected from the three motors each run under several inverter-frequencies. To provide a holistic view of the fault signature database, each FFT-ICA feature, which obtained by using Eqn. 13, is normalized using the healthy motor as a benchmark for comparing with faulty condition. The performance of the proposed method is demonstrated by comparing to the existing frequency analysis based methods and our previous time-domain method.

1) Comparison with Conventional Frequency Analysis Methodd: Fault frequency of the motor with bearing fault can be obtained as shown in Table II by using the parameters in Table I and Table II. The bearing fault frequency signatures changes with the supply frequency as shown in Table II. We can locate the bearing fault frequency according to Table II as shown in Fig. 3.

Similarly, the fault frequency of the motor with broken rotor bar can be estimated by using the obtained parameters shown in Table III according to Eqn. 3. The broken rotor fault signature frequency (sidebands) changes with the supply frequency as shown in Table III. Table II and Table III also shows that the bearing fault frequency signatures are located in higher frequency band compared to fault signatures of broken rotor bars.

However, without using the measurement of the slip or parameters of the motors, our proposed method can give perfect classification results as shown in Fig. 4(b).

2) Comparison with the Previous Time-domain Analysis Method: Fig. 4 shows performance of our proposed method compared with the previous time-domain ICA method. Under each inverter frequency, our proposed frequency-domain ICA method give better results than time-domain ICA method, and there is no drifting (Fig. 4(a)) of the two faulty cluster with changing inverter frequency as shown in Fig. 4(b).

The proposed algorithm involves simply partial substitution of the new signal into Eqn. 15 for calculating the FFT-ICA features. The features directly show the type of the motors. Unlike our previous time-domain ICA method for fixed frequency [12] and hybrid time-frequency domain analysis method [14], a fuzzy neural network (FNN) or a fuzzy system (FS) are not required for the presently proposed algorithm. The fault detection would be 100% accurate judging from the superior performance of the classification as shown in Fig. 4(b).

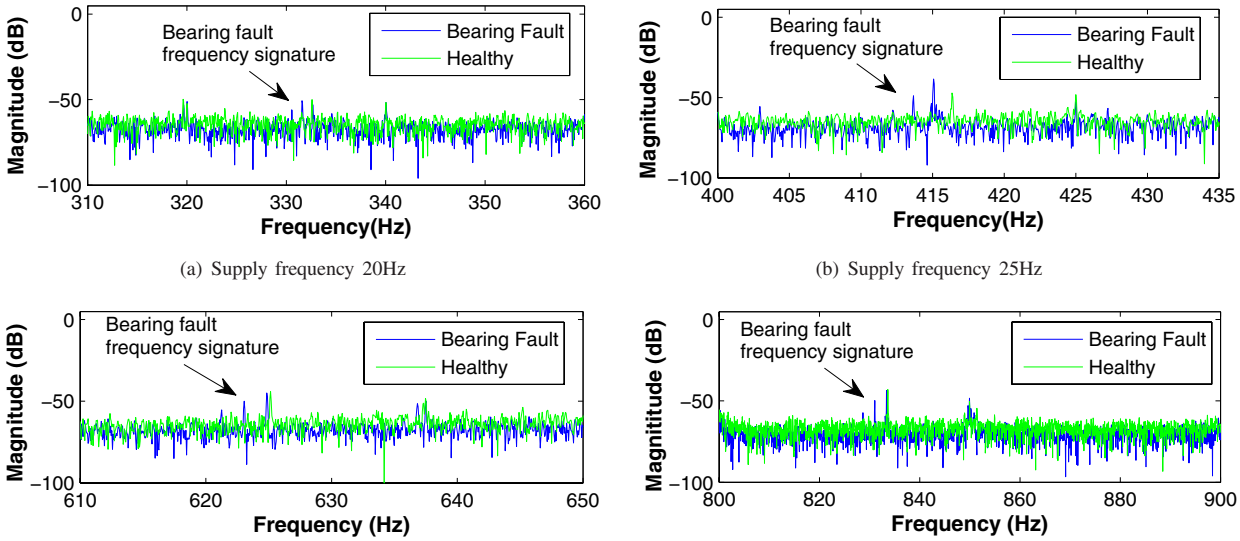

(a) Supply frequency 20Hz

(b) Supply frequency 25Hz

(c) Supply frequency 37.5Hz

(d) Supply frequency 50Hz

Fig. 3. Locating bearing fault frequency signatures using the parameters in Table I.

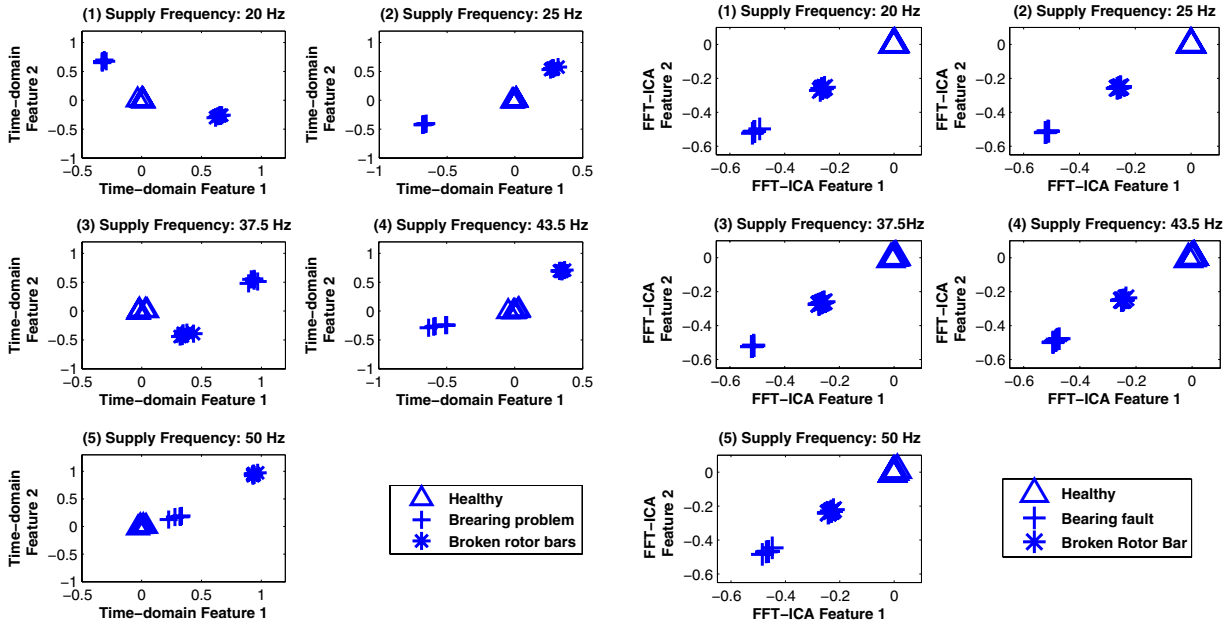

(a)

(b)

Fig. 4. Comparison between previous time-domain method and the proposed frequency-domain feature based method at each frequency supply: (a) Results obtained by time-domain method under supply frequency: 20Hz, 25Hz, 37.5Hz, 43.5Hz and 50Hz; (b) Results obtained by frequency-domain feature based method under supply frequency: 20Hz, 25Hz, 37.5Hz, 43.5Hz and 50Hz

TABLE III
NECESSARY PARAMETERS NEEDED AND ESTIMATED FAULT FREQUENCY OF THE MOTOR WITH BROKEN ROTOR BARS

Supply Frequency (Hz)	Measured/ Estimated Rotor Speed (rpm)	Per-unit slip	Broken Rotor Bar Fault Signature Frequency f_b (Hz)
20.0	582/600	0.0300	18.81/21.16
25.0	729/750	0.0280	23.60/26.40
37.5	1095/1125	0.0267	35.43/39.47
43.5	1271/1305	0.0261	41.23/45.76
50.0	1461/1500	0.0260	47.41/52.59

V. CONCLUSION

A new algorithm for the fault detection of induction motor is presented and the mathematical formulation is developed to utilize FFT and ICA to calculate the features of the stator-current signals. The features obtained in the present way are shown to have the content of the motor's fault information. Compared with our existing time-domain ICA method and conventional frequency domain analysis techniques, our proposed scheme provides more robust, flexible, reliable and easy-to-implement fault detection on induction motors under varying frequency.

ACKNOWLEDGMENT

The authors would like to thank National University of Singapore for supporting their research work.

REFERENCES

[1] M. Benbouzid, "Review of induction motors signature analysis as a medium for faults detection," *IEEE Transactions on Industrial Electronics*, vol. 47, no. 5, pp. 984–993, 2000.

[2] W. Thomson and M. Fenger, "Current signature analysis to detect induction motor faults," *IEEE Industry Applications Magazine*, vol. 7, no. 4, pp. 26–34, 2001.

[3] A. Bellini, F. Filippetti, G. Franceschini, C. Tassoni, and G. Kliman, "Quantitative evaluation of induction motor broken bars by means ofelectrical signature analysis," *IEEE Transactions on Industry Applications*, vol. 37, no. 5, pp. 1248–1255, 2001.

[4] C. Cunha, R. Lyra, and B. Filho, "Simulation and analysis of induction machines with rotor asymmetries," *IEEE Transactions on Industry Applications*, vol. 41, no. 1, pp. 18–24, 2005.

[5] B. Ayhan, M. Chow, and M. Song, "Multiple signature processing-based fault detection schemes for broken rotor bar in induction motors," *IEEE Transactions on Energy Conversion*, vol. 20, no. 2, p. 336, 2005.

[6] H. Su and K. Chong, "Induction machine condition monitoring using neural network modeling," *IEEE Transactions on Industrial Electronics*, vol. 54, no. 1, pp. 241–249, 2007.

[7] B. Ayhan, M. Chow, and M. Song, "Multiple discriminant analysis and neural-network-based monolith and partition fault-detection schemes for broken rotor bar in induction motors," *IEEE Transactions on Industrial Electronics*, vol. 53, no. 4, p. 1298, 2006.

[8] K. Bimal, "Power Electronics and Motor Drives Recent Progress and Perspective," *IEEE Transactions on Industrial Electronics*, vol. 56, no. 2, pp. 581–588, 2009.

[9] M. Khan and M. Rahman, "Development and implementation of a novel fault diagnostic and protection technique for IPM motor drives," *IEEE Transactions on Industrial Electronics*, vol. 56, no. 1, pp. 85–92, 2009.

[10] F. Zidani, D. Diallo, M. El Hachemi Benbouzid, and R. Nait-Said, "A fuzzy-based approach for the diagnosis of fault modes in a voltage-fed PWM inverter induction motor drive," *IEEE Transactions on Industrial Electronics*, vol. 55, no. 2, pp. 586–593, 2008.

[11] O. Alejandro, R. de Jesus, V. Alberto, R. Rooney, and G. Arturo, "Automatic online diagnosis algorithm for broken-bar detection on induction motors based on discrete wavelet transform for FPGA implementation," *IEEE Transactions on Industrial Electronics*, vol. 55, no. 5, pp. 2193–2202, 2008.

[12] Z. Wang, C. S. Chang, X. German, and W. W. Tan, "Online Fault Detection of Induction Motors Using Independent Component Analysis and Fuzzy Neural Network," in *8th IET International Conference on Advances in Power System Control, Operation and Management, Hong Kong*, 2009.

[13] Z. Wang, C. S. Chang, T. Chua, and W. W. Tan, "Ensemble and Individual Noise Reduction Method for Induction-motor Signature Analysis," in *8th IET International Conference on Advances in Power System Control, Operation and Management, Hong Kong*, 2009.

[14] T. Chua, W. W. Tan, Z. Wang, and C. S. Chang, "Hybrid Time-Frequency Domain Analysis for Inverter-Fed Induction Motor Fault Detection," in *IEEE International Symposium on Industrial Electronics, ISIE*, 2010.

[15] S. Nandi, R. Bharadwaj, and H. Toliyat, "Performance analysis of a three-phase induction motor under mixed eccentricity condition," *IEEE Transaction on Energy Conversion*, vol. 17, no. 3, pp. 392–399, 2002.

[16] B. Akin, U. Orguner, H. Toliyat, and M. Rayner, "Low order PWM inverter harmonics contributions to the inverter-fed induction machine fault diagnosis," *IEEE Transactions on Industrial Electronics*, vol. 55, no. 2, pp. 610–619, 2008.

[17] M. Benbouzid and G. Kliman, "What stator current processing-based technique to use for induction motor rotor faults diagnosis?" *IEEE Transaction on Energy Conversion*, vol. 18, no. 2, pp. 238–244, 2003.

[18] J. Jung, J. Lee, and B. Kwon, "Online diagnosis of induction motors using MCSA," *IEEE Transactions on Industrial Electronics*, vol. 53, no. 6, pp. 1842–1852, 2006.

[19] D. Tsai and S. Lai, "Independent component analysis-based background subtraction for indoor surveillance," *IEEE Transactions on Image Processing*, vol. 18, no. 1, pp. 158–167, 2009.

[20] A. Irimia, W. O. Richards, and L. A. Bradshaw, "Comparison of conventional filtering and independent component analysis for artifact reduction in simultaneous gastric emg and magnetogastrography from porcines," *IEEE Transactions on Biomedical Engineering*, vol. 56, no. 11, pp. 2611 –2618, 2009.

[21] C. S. Chang, J. Jin, C. Chang, T. Hoshino, M. Hanai, and N. Kobayashi, "Online source recognition of partial discharge for gas insulated substations using independent component analysis," *IEEE Transactions on Dielectrics and Electrical Insulation*, vol. 13, no. 4, p. 892, 2006.

[22] A. A. Amanatiadis and I. Andreadis, "Digital image stabilization by independent component analysis," *IEEE Transactions on Instrumentation and Measurement*, vol. 59, no. 7, pp. 1755 – 1763, 2010.

[23] M. Crespo-Garcia, M. Atienza, and J. Cantero, "Muscle artifact removal from human sleep EEG by using independent component analysis," *Annals of Biomedical Engineering*, vol. 36, no. 3, pp. 467–475, 2008.

[24] A. Widodo, B. Yang, and T. Han, "Combination of independent component analysis and support vector machines for intelligent faults diagnosis of induction motors," *Expert Systems with Applications*, vol. 32, no. 2, pp. 299–312, 2007.